

Stability analysis and speed control of brushless DC motor based on self-ameliorate soft switching control methods

Nagaraja Rao¹, Shantharama Rai Chelladka²

¹Department of Electronics and Communication Engineering, Faculty of Engineering, Shri Madhwa Vadiraja Institute of Technology and Management, Udupi, India

²Department of Electronics and Communication Engineering, Faculty of Engineering, AJ Institute of Engineering and Technology, Mangalore, India

Article Info

Article history:

Received Nov 12, 2021

Revised Oct 2, 2022

Accepted Dec 2, 2022

Keywords:

Brushless direct current motor
Driver circuit
Self-ameliorate soft switching
speed sensor
Torque-speed characteristics

ABSTRACT

In recent years, electric vehicles are the large-scale spread of the transportation field has led to the emergence of brushless direct current (DC) motors (BLDCM), which are mostly utilized in electrical vehicle systems. The speed control of a BLDCM is a subsystem, consisting of torque, flux hysteresis comparators, and appropriate switching logic of an inverter. Due to the sudden load torque variation and improper switching pulse, the speed of the BLDCM is not maintained properly. In recent research, the BLDC current control method gives a better way to control the speed of the motor. Also, the rotor position information should be the need for feedback control of the power electronic converters to varying the appropriate pulse width modulation (PWM) of the inverter. The proposed optimization work controls the switching device to manage the power supply BLDCM. In this proposed self-ameliorate soft switching (SASS) system is a simple and effective way for BLDC motor current control technology, a proposed control strategy is intended to stabilize the speed of the BLDCM at different load torque conditions. The proposed SASS system method is analyzing hall-based sensor values continuously. The suggested model is simulated using the MATLAB Simulink tool, and the results reveal that the maximum steady-state error value achieved is 4.2, as well as a speedy recovery of the BLDCM's speed.

This is an open access article under the [CC BY-SA](https://creativecommons.org/licenses/by-sa/4.0/) license.



Corresponding Author:

Nagaraja Rao

Department of Electronics and Communication Engineering, Faculty of Engineering, Shri Madhwa Vadiraja Institute of Technology and Management

SMVITM, Bantakal, Udupi, India

Email: nagarajsmvitm1@gmail.com

1. INTRODUCTION

Recently, brushless direct current motors (BLDCM) have gained so much interest due to their simple control and easy maintenance. In other motors, the brushless direct current (DC) motor about torque pulsation shows better performance than the traditional positioning counterparts. This characteristic comes from the low cogging torque of the brushless DC motor. The BLDCM has numerous features such as linear torque-speed characteristics and easiest control arrangements, which do not necessitate complex hardware. The hall sensor-based speed control of the BLDCM is shown in Figure 1.

In this work, Xia and Gao [1] presented that self-ameliorate soft switching (SASS) reduces the torque ripple and the speed control of the BLDC motor. The typical method is pulse width modulation (PWM) control plus a continuous control scheme. By controlling the current-based control structure the hysteresis controller is utilized. Both of these systems have a high current control since the value of the controlled variable is forced

away from the surrounding reference value within certain limits. However, it is difficult to apply to the device because this technology has a short hysteresis band ripple when the high switching frequency and large hysteresis band are wide and uncontrollable. In contrast, the PWM current control with a lower current control, but it has the advantage of a constant frequency switching device. Thus, the PWM method is suitable for low hysteresis current control transistor switching losses and the power ratio. Moreover, the acoustic and electromagnetic noise filter is relatively easy since the frequency is stable.

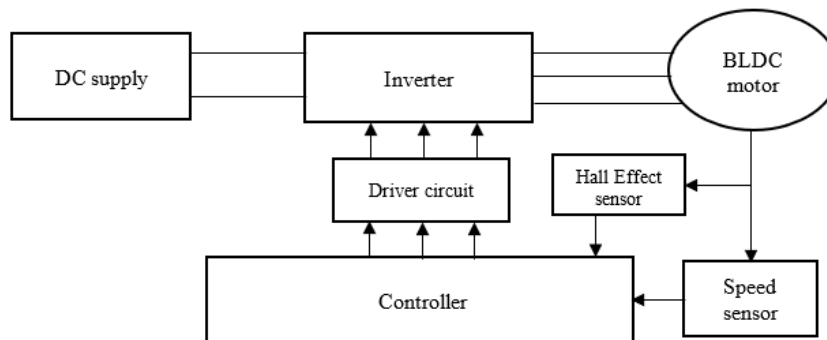


Figure 1. Functional block diagram for the BLDCM

As described above, the control voltage source inverter variable speed drive stability plays a key role, cost minimization is becoming one of the proposed DC brushless motor control systems of most important issues. In this system, a three-phase AC inverter drive is mainly applied and has certain advantages since, for example, in a power transistor, conduction loss is reduced, reducing the number of the easier control algorithm, to generate a switching signal. The appropriate switching signal will maintain the speed control of the BLDCM. The SASS system provides a stability control operation of the BLDC motor. with this analysis the various features like rise time (seconds), less settling time (seconds), and maximum overshoot (seconds) is obtained with an effective ratio.

2. LITERATURE SURVEY

The growing demand for motorized applications such as electric vehicles and industrial automation has led to increased interest in BLDCM due to their relatively small size and performance [2]. It proposes a coordinated optimal shift control system for electric motor torque control, a two-speed gearbox introduced in the process of slip clutch in electric vehicles. Among these, the torque of the motor and clutch thrust signals are input to the optimized controller [3], [4]. A robust sliding mode controller (RSMC) was structured, and the guided control law is separated into two sections: continuous and discontinuous. Delay problems with linear quadratic regulators (LQRs) and networks have established goals to reduce reference state tracking errors and reduce the control strength of the BLDCM [5]. Specifically, some safety regulation formulations for charging electric vehicles (EVs) to ensure electrical safety and prevent dangerous accidents. Among them, the requirements for need battery safety for electric vehicles are the two main driving factors. When connected to renewable energy generation [4], the comprehensive system for assessing the electrical safety of large electrical vehicle fast charging simplified (EVCSs). For mobile EVs, the only viable solution for electromagnetic energy charging, inductive power transfer (IPT) cannot compare with other technologies, static offers the possibility and includes dynamic charging [6].

The advantages of steering controllers for path tracking together with torque vectors [7] and path tracking controllers are used in autonomous electric vehicles, either through integrated torque systems or through separate implementations. A safe driving and control system is connected to automatically accelerating or securing a vehicle safety constraint while optimizing deceleration [8]. It proposes an optimal method for any type of charge depletion mode for versatile vitality utilization minimization methodology module of the electric vehicle [9]. The adaptive sliding mode fault tolerant coordination (ASMFC) controller is used for speed control of BLDCM. The sliding mode controller will analyze the speed at different time responses [10].

The dynamic remote force charging innovation of electric vehicles is a transmitter curl, which is put under the ground. At the point when the electric vehicle and the getting should be overloaded the hysteresis current controller should be regulate and stabilize the speed [11] to realize the wireless dynamic charging of the vehicle, a modular multi-level converter (MMC) with basic embedded units, integrated balance function

represents an effective alternative of the EV system [12]. The development of electric vehicles features the charging network business market and forms, including the internet of things based communication system [13] charging network policy. The hybrid energy storage system (HESS), along with high power density ultra-capacitors, consists of high energy density battery packs. Motor drives for internal permanent magnet (IPM) motors are usually designed depends on a fixed DC bus voltage [14].

To exploit this consecutive drive repetition to decrease machine corruption while guaranteeing that the necessary shut circle execution [15]. It proposes another switched reluctance motor (SRM) with a wide speed extend for EV applications [16]. Electric motors are generally reasonable for vehicle applications since they can grow high beginning forces. This prompted the improvement of batteries for working EVs, In-wheel operation of the wheel, and energy component vehicles [17]. Brushless DC motors are three-phase permanent magnet motors and require a DC voltage as their power source [18].

Transportation is the principle segment that produces human wellbeing and air contamination, which is poisonous to the reasons for an unnatural weather change. Air contamination can be limited by utilizing sustainable power sources and propelled electric engines for inside ignition motor transportation [19]. Accurate analysis of vehicle performance is required, including dynamic models of many components such as its electric motor, its battery, and its motor controller [20]. Another regenerative braking system (RBS) has been proposed for use in the EV and is driven by a brushless DC motor. During regenerative slowing down, BLDC is act as a generator [21]. To meet the endless fuel demands of vehicles, research on hybrid vehicles with the wireless battery charging system [22]. For high-efficiency energy recovery and safety series of hybrid electric vehicles, the integrated braking system has a subsystem and advanced power consumption braking strategy are utilized [23], [24]. In the open loop control of BLDC motor, speed is set to reference value, whereas in closed loop control this is varied at any given time for the operation at desired speed. It is observed that, BLDC motor running with fixed speed without having any significant ripples in torque. With the PI controller for closed loop operation, performance of the motor has been modeled for the varying load [25], [26].

3. PROPOSED SYSTEM

The general structure of the proposed dynamic rule-based vector formed control fed BLDCM drive model is showed up in Figure 2. It comprises of BLDCM, Inverter, position resolver, and controller. The speed controller controlled BLDCM drives the feedback circuit in the external circuit, and the coordinated vector current driver, which produces an effective result. When the phase current is detected at the time of measurement, the current part of the torque and magnetic flux is gained through the coordinate transformation. Then, the two currents are compared to a predetermined reference value, and through a single proportional integral (PI) current controller, which determines the error handling nominal voltage at the motor terminals. The actual speed of the motor is sensed and related with a reference value command. The rate error is processed by the SASS speed controller, which determines the reference and the determined set point from the fuzzy rule. The proposed SASS speed controller combines the benefits of fuzzy controllers.

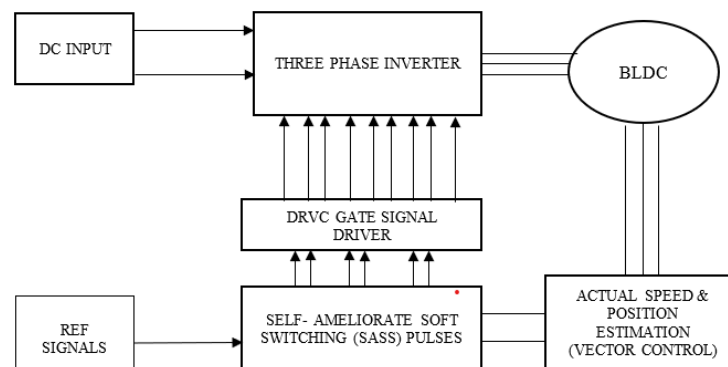


Figure 2. Proposed block for speed control BLDCM

The load torque variation-based switching function is executed in a simulation model based on the selected error value when the start time of the fuzzy controller. In running operation, the SASS controller to provide better performance to vary the PWM signal according to the error ratio. Based on the error value inverter will varying the speed of the BLDCM. During the movement, the transfer switch determines the SASS controller to provide improved performance.

3.1. Modeling of BLDCM

Modeling of BLDCM can be developed similarly to three-phase synchronous motors. Due to the permanent magnets installed on its rotor, some dynamic properties of the BLDCM are a different form of synchronous motor. The flux linkage from the rotor depends on the magnet. Thus, the saturation magnetic flux linkage is characteristic of such a motor. The typical structure of the voltage source inverter (VSI) fed BLDCM is shown in Figure 3.

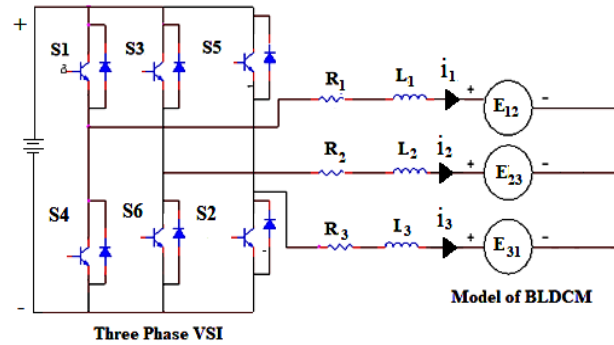


Figure 3. Three phase inverters based BLDCM

The armature modeling equation of BLDCM is expressed (1) to (3).

$$V_1 = Ri_1 + L_1 \frac{di_1}{dt} + E_{12} \quad (1)$$

$$V_2 = Ri_2 + L_2 \frac{di_2}{dt} + E_{23} \quad (2)$$

$$V_3 = Ri_3 + L_3 \frac{di_3}{dt} + E_{31} \quad (3)$$

Or the compact matrix form is (4).

$$\begin{bmatrix} V_1 \\ V_2 \\ V_3 \end{bmatrix} = \begin{bmatrix} R + pL & 0 & 0 \\ 0 & R + pL & 0 \\ 0 & 0 & R + pL \end{bmatrix} \begin{bmatrix} i_1 \\ i_2 \\ i_3 \end{bmatrix} + \begin{bmatrix} E_{12} \\ E_{23} \\ E_{31} \end{bmatrix} \quad (4)$$

where the L_1, L_2, L_3 is self-inductance and the R represents the armature resistance, also $V_1, V_2, V_3 =$ terminal voltage, $i_1, i_2, i_3 =$ motor input current in ampere and $E_{12}, E_{23}, E_{31} =$ motor back emf in volts. p in the matrix represents $\frac{d}{dt}$.

The modified back EMF must be expressed (5) to (7).

$$E_{12}(t) = K_e \phi(\theta) \omega(t) \quad (5)$$

$$E_{23}(t) = K_e \phi\left(\theta - \frac{2\pi}{3}\right) \omega(t) \quad (6)$$

$$E_{31}(t) = K_e \phi\left(\theta + \frac{2\pi}{3}\right) \omega(t) \quad (7)$$

where in, K_e is the back electromotive force constant, ω is the mechanical speed of the brushless DC motor. It generates a torque that also affects the permanent magnet flux is a trapezoid.

$$T_e = \frac{(E_1 i_1 + E_2 i_2 + E_3 i_3)}{\omega} \quad (8)$$

The torque T_e can be gained by the subsequent expression,

$$T_1(t) = K_T * \phi(\theta) * i_1(t) \quad (9)$$

$$T_2(t) = K_T * \phi \left(\theta - \frac{2\pi}{3} \right) * i_2(t) \quad (10)$$

$$T_3(t) = K_T \phi * \left(\theta + \frac{2\pi}{3} \right) * i_1(t) \quad (11)$$

$$T_E(t) = (T_1(t) + T_2(t) + T_3(t)) \quad (12)$$

where, K_T is the torque constant. The angular motion of the rotor can be expressed (13).

$$T_e(t) = T_L(t) = J \frac{d\omega(t)}{dt} + B * \omega(t) \quad (13)$$

where, $T_L(t)$ is load torque in N-m, J is rotor inertia in $[[kgm]]^2$, and B is damping constant

3.2. Self-ameliorate soft switching based closed-loop speed control operation

The Brushless DC motors can be controlled by controlling a three-phase inverter using SASS switching pulses. Provides data about the required speed and torque values during an error condition in the control unit. The BLDC motor drive control is used SASS as a switching controller which consists of three main components, namely fuzzification, defuzzification, and dynamic rule decision logic interface. In Figure 4, shows the input data is converted into suitable language variables. The input and output variable estimates are numerical variables, and the resulting variable estimates are semantic factors, for example, negative big factor (NBF), negative average factor (NAF), negative small factor (NSF), zero (Z), positive small factor (PSF), positive average factor (PMF) and positive big factor (PBF).

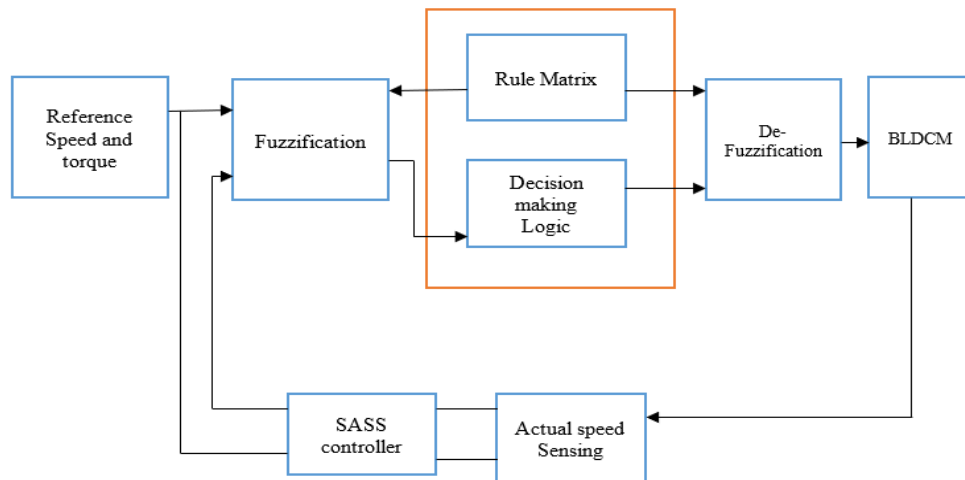


Figure 4. SASS closed-loop block diagram

3.2.1. Fuzzification

Fuzzification is the first step in applying fuzzy inference systems. Most of the existing actual variables (reference speed and torque) are scalable variables (reference speed). Those desired variables (input and output) are converted into desired fuzzy variables, and then from the application to improve the SASS to process the data inference to obtain the desired output. Finally, in most cases, those fuzzy output variables need to be converted back to the desired, in order to achieve the desired control objectives.

The triangular membership function is assigned to the input and output variables. As a function of the error variable normalized interval $[-1.1, 1.1]$. The universe of discourse changes in the error function is normalized in the interval $[-0.04, 0.04]$. Figure 5 shows the input membership functions.

3.2.2. Decision making logic

Input-output relational language choice rules are summarized in Table 1. The reasoning engine carries out the instructions for Rule 49 (77), and it then processes the variables. MATLAB's fuzzy logic tools (FTL) are used to do an interpretation of the rules based on the tables that were created for the rules' creation.

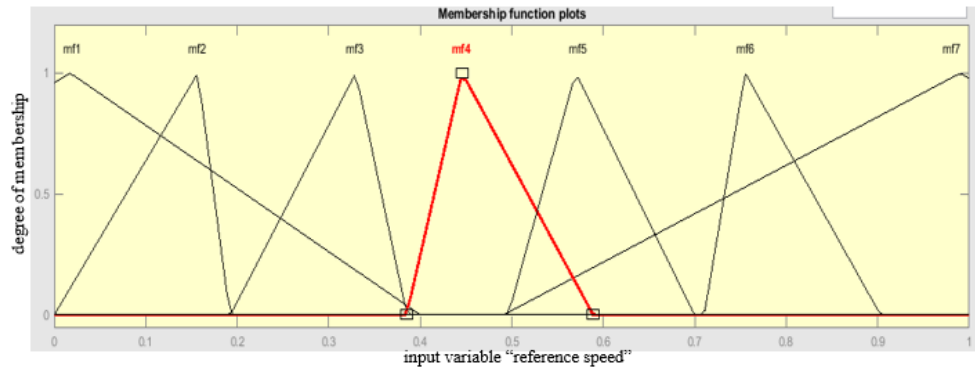


Figure 5. Membership function of the input variables

Table 1. Decision table rule base

Rule	Error e(k)							
	NBF	NMF	NSF	ZEF	PSF	PMF	PBF	
Change in error Ce (k)	NBF	NBF	NBF	NBF	NMF	NSF	ZE	
	NMF	NBF	NBF	NM	NS	ZE	PS	
	NSF	NBF	NMF	NSF	ZE	PSF	PMF	
	ZE	NB	NM	NS	ZE	PM	PB	
	PSF	NMF	NSF	ZE	PSF	PMF	PBF	
	PMF	NSF	ZE	PSF	PMF	PBF	PBF	
	PBF	ZE	PSF	PMF	PBF	PBF	PBF	

3.2.3. De-fuzzification

In order to make this conclusion or fuzzy output available in practical applications, a clear process is needed. The defuzzification process converts the fuzzy outputs of classical or standard output back to the control target. The fuzzy conclusion or output is still a linguistic variable, which needs to be converted into a standard variable in the defuzzification process. Figure 6 shows the output membership function.

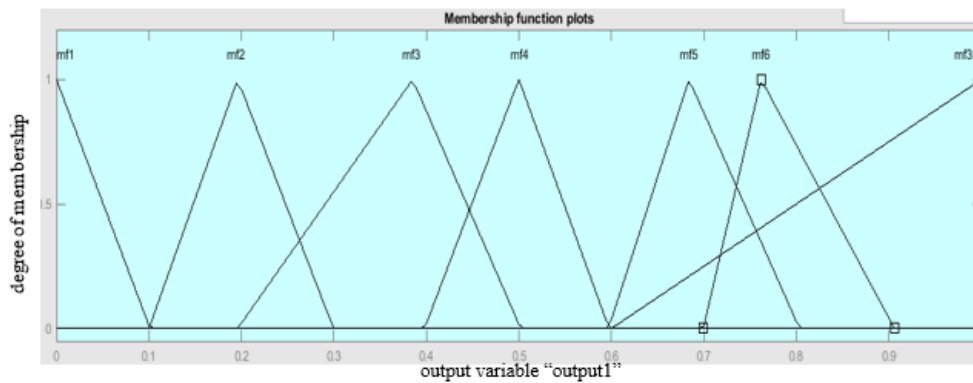


Figure 6. Output membership functions

3.3. SASS controller-based inverter control system

BLDC motor is operated based on a six-step commutation sequence or 120°-degree conduction mode to generate switching pulses for power switches in the inverter. At any time, only two phases of the motor are energized, and the other phase is in a floating state. This calculation logic helps the trapezoidal BLDCM counter electromotive force. Table 2 shows the six switching states used to generate commutation logic for BLDC motor. In the general driving circuit of a BLDC motor is a three-phase inverter as shown in Figure 7. From the Table 2 can observe that at any instant only two switches conduct, and each switch conducts for an interval of 120°. The corresponding phase current showed in Table 2 for six switching states shows that at every 60-degree interval one phase current is zero.

Table 2. Switching Table for BLDC motor

Hall Signal			ON Switch		Line Current Sign		
A	B	C			Phase A	Phase B	Phase C
0	0	1	S1	S6	1	0	-1
0	0	0	S1	S4	1	-1	0
1	0	0	S4	S5	0	-1	1
1	1	0	S2	S5	-1	0	1
1	1	1	S3	S2	-1	1	0
0	1	1	S3	S6	0	1	-1

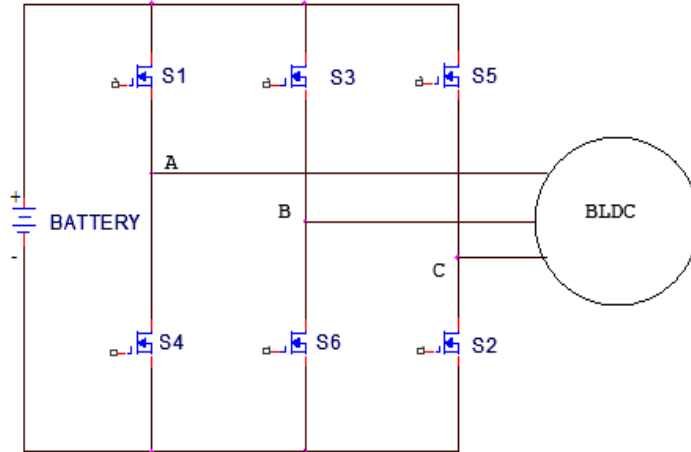


Figure 7. Circuit for three-phase inverter driving BLDC motor

In the first switching step top switch of leg A and bottom switch of the leg, C conducts and the R phase current is positive and the B phase current is negative. In the next switching step top switch of leg A and bottom switch of leg B conducts and the R phase current is positive and the Y phase current is negative. In the next switching step top switch of leg C and bottom switch of leg B conducts and the B phase current is positive and the Y phase current is negative. In the next switching step top switch of leg C and bottom switch of leg A conducts and the B phase current is positive and the R phase current is negative. In the next switching step top switch of leg B and bottom switch of the leg, C conducts and the Y phase current is positive and the B phase current is negative. In the next switching step top switch of leg B and bottom switch of leg A conducts and the Y phase current is positive and the R phase current is negative.

3.4. Self-ameliorate soft switching control algorithm

In this work, it will be shown that SASS techniques can also be used useful in applications, where traditional controls perform well. The Fuzzy logic allows for simpler and more robust control solutions whose performance can only be matched by traditional controllers. In this work, the fuzzy speed controller is replaced with a SASS to improve the performance of the BLDCM.

The SASS controller uses speed tracking error and its change as input and generates reference torque as output. The input signal is defined (14) and (15).

$$= \omega^*(k) - \omega_{actual}(k) \tag{14}$$

$$Ce(k) = \omega_{error}(k) - \omega_{error}(k - 1) \tag{15}$$

where, $\omega^*(k)$ is the set speed of the BLDCM; $\omega_{actual}(k)$ is the speed of the motor at k^{th} -samples; $Ce(k)$ is the changing in error at k^{th} -samples.

In order to improve the sensitivity of control, the quantization factor used for the actual value of the error and its change is quantified, and then they are mapped to the fuzzy set domain $X=\{-m, -m+1, \dots, 0, \dots, m+1, \dots, 0, m-1, \dots, m\}$. The performance of the system will be improved by the determination of the SASS control rules as the result of increasing difficulty m which is the larger value. In this work, the value of m is used as a pair of errors and changes in error $Ce(k)$. The output signal from the fuzzy domain is converted into a base structure domain or actual output by using the scaling factor so that the output can be used to control the system.

3.4.1. SASS algorithm steps

- Step 1: Initializing a set of predefined error e , and then mapped to the fuzzy set domain X value & Center; A) Error b) error rate (variation of error) and set domain.
 - Step 2: Fuzzy set formation
Fuzzy set example, NBF, NAF, NSF, Z, PSF, and PMF, and PBF.
 - Step 3: Fuzzy calculation of the membership degree of each fuzzy set input.
 - Step 4: Compute the error $\omega_{error}(k)$,
 - Step 5: The actual value of the error and its change are quantified, and then they are mapped to the fuzzy set domain $X=\{-m, -m+1, \dots, 0, \dots, M+1, \dots, 0, m-1, \dots, m\}$.
 - Step 6: The performance of the system will be determined by a control rule difficulty SASS increased m a result a large value.
 - Step 7: Choose candidate branch u_j in order from the discrete control set $\{S_0, S_1, \dots, S_6\}$, where $j= 1, 2, \dots, 7$, then calculate predictive node $x_j(k+m)$, finally $m=m+1$.
 - Step 8: If $m < F$, go back to step 4); else, go to the next step.
 - Step 9: Calculate the each of the negative branch $u_j(k+m-1)$ in order by equation, where $j= 0, 1, \dots, 7$, then calculate the momentum function J_{k+m} on the basis F, I, V weighs matrices and previous J_{k+m+1} (if $m=F, J_{k+m+1}=0$). Minimize J_{k+m} to select the optimal input $u^*(k+m-1)$ and determine SASS control signal sequence $U^*(k+m-1)$. Finally, $m=m-1$.
- where,
 $(k+m-1)$ = Negative node rotor angle compare with the modulation index
 J_{k+m} = inertia of the motor with modulation index
 $m= F$ is the modulation index with inverter frequency
 $U^*(k+m-1)$ = SASS control signal sequence of the inverter
- Step 10: Apply the first optimal input $u^*(k)$ to the BLDCM system.
End this algorithm.

Figure 8 provides an explanation of the control processes followed by the SASS controller while the BLDCM speed control operation is being performed. The set speed and reference speed are both determined by the SASS controller in this control module. Their determination is dependent on the value that will be changed by the inverter PWM.

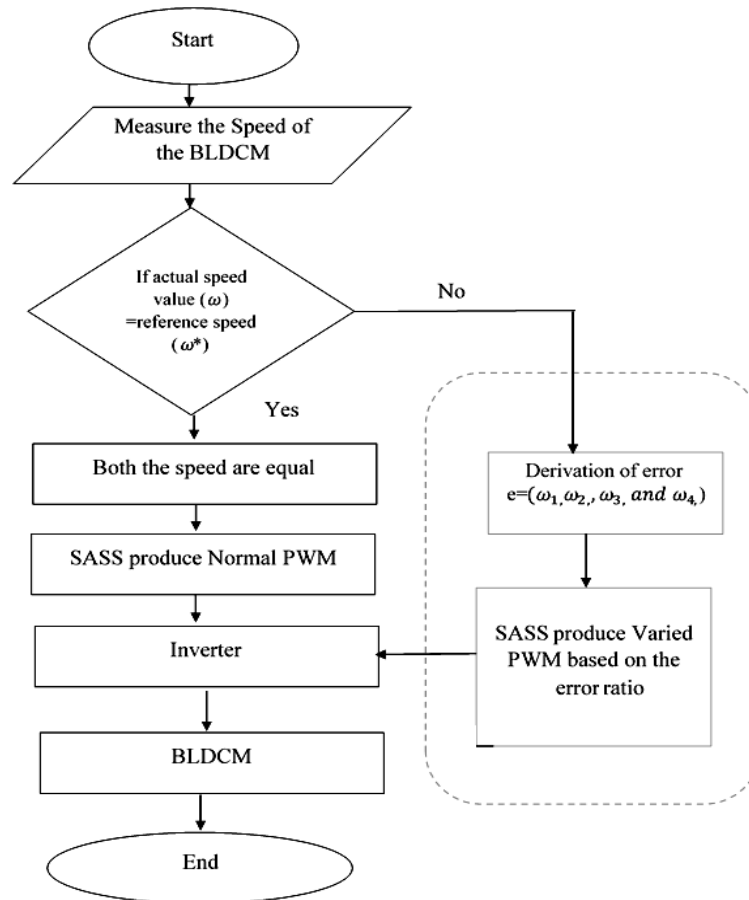


Figure 8. The flow diagram for the SASS based BLDCM

4. RESULTS AND DISCUSSION

This proposed method of induction motor driver system utilizing MATLAB2017b software is to be used and simulate the system function and coordinated into the simulation model of a SASS system. The implementation of the proposed model in MATLAB/Simulink, the use of the system, and the ability to display libraries SIM power supply system-wide settings BLDCM proof, which is seen in Figure 9. The overall Simulink model has given the BLDC motor controlling strategy. The DC source is given to the system, and the converter is given to the supply of the motor. The proposed SASS system is used to control the system's power. It is shown in Figure 9. The system torque, phase current, and flux are analyzed in this system.

Figure 10 gives the system output current of the BLDC motor. The proposed SASS control system performance is improved. The torque is applied at 0.2 seconds, due to this, the stator current is maintained at 0.2 seconds.

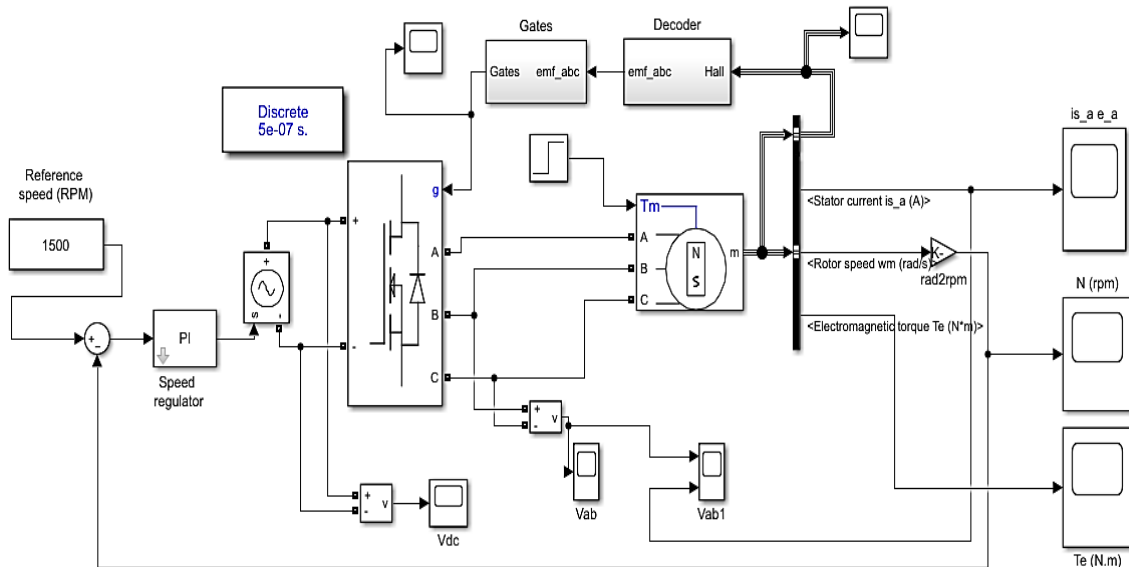


Figure 9. Proposed system Simulink model

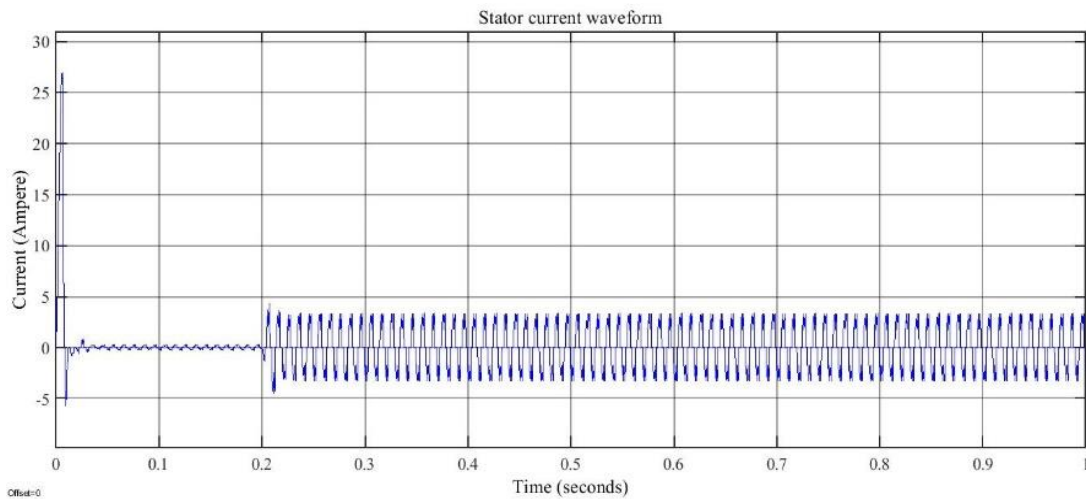


Figure 10. Output current of the proposed system

Figure 11 shows the BLDC motor torque. For the differential speed analysis of the load, torque is applied at the time duration of 0.2 seconds, based on the torque value, the speed and stator currents are varied. Figure 12 gives the system speed of the BLDC motor. Using the proposed SASS controller, stabilize the speed

of the BLDC at 1500 RPM due to the load torque variation at the time of 0.2 seconds the speed of the BLDCM is slightly varied the proposed SASS controller is the quick recovery of the speed of the BLDCM. To analyze the different parameters, for example, recovery time, and peak overshoot time, steady-state error to compare the performance BLDCM. From the simulation, the test is arranged in Table 3 and the results show that the SASS-based controller provides better results.

The control system parameters for varying different load torque condition conditions are represented in Table 3 and Figure 13. The system will compare with the proposed SASS controller. When compared to other conventional techniques, the proposed method gives a perfect result. From all of the above analysis, the assignment SASS control method proposed various parameters that have been evaluated and compared to other conventional methods that have produced results accuracy.

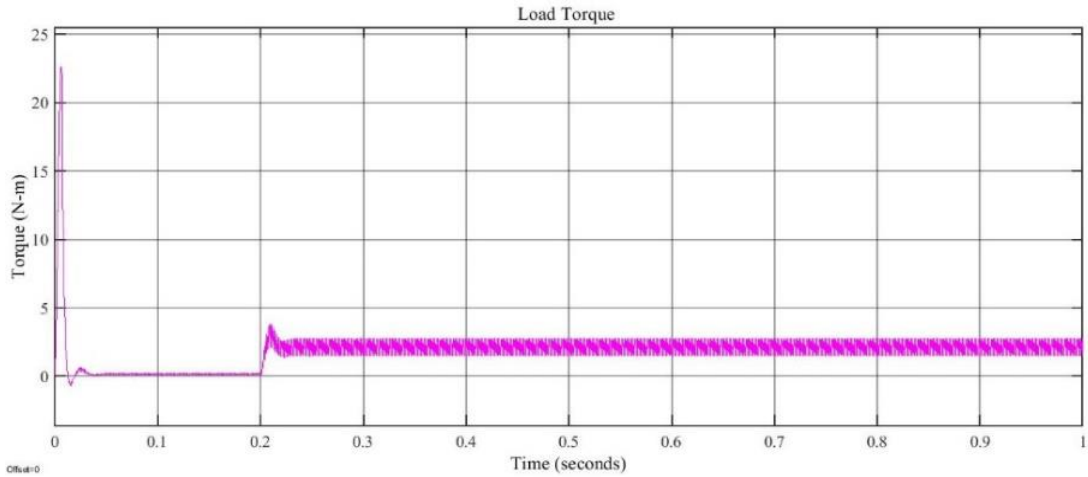


Figure 11. BLDC motor torque

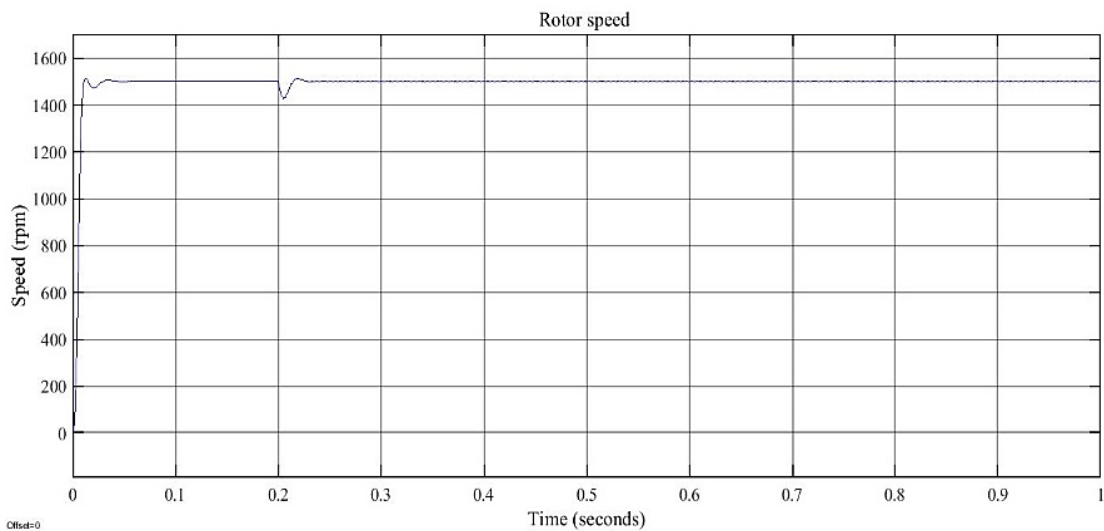


Figure 12. BLDC motor speed

Table 3. Comparing the performance parameters of The BLDC motor

Methods	Reference Value (RPM)	Peak Overshoot Time (sec)	Recovery Overshoot (%)	Recovery Time (sec)	Steady State Error Value (RPM)	Steady State Error (%)
PID	1500	0.6417	0.7632	0.66	9.25	0.69
Fuzzy	1500	0.6010	0.5423	0.60	6.25	0.52
SASS	1500	0.9563	0.4231	0.41	4.2	0.36

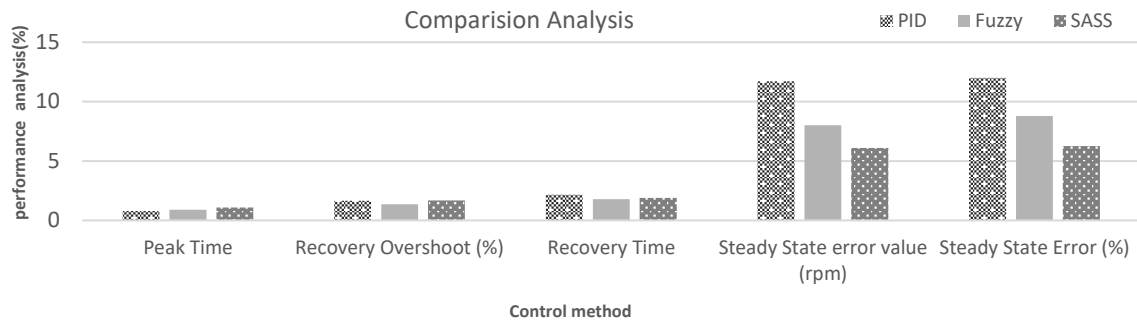


Figure 13. Comparison analysis

5. CONCLUSION

This work introduces the modeling and simulation of the photovoltaics (PV) fed BLDC based water pumping system with a controller, namely the SASS. The performance of the controllers has been validated using MATLAB, and detailed analyses of all the parameters are presented. With this special model results are obtained from simulation; it is clear that for the improvise operating condition for the BLDC speed control; the steady-state value is 5.8% which is better than the existing controller. From the summary of results, it can be presumed that error elimination and complete reduction of steady-state error are the unique features of the proposed SASS controllers. The constant speed operation ensures the constant operation of the automotive way. The advanced SASS control produces the maximum steady-state error value is 4.2.




REFERENCES

- [1] C. Xia and G. Gao, "Brushless DC motors control based on smith predictor modified by fuzzy-PI controller," in *2008 Fifth International Conference on Fuzzy Systems and Knowledge Discovery*, Oct. 2008, pp. 289–293, doi: 10.1109/FSKD.2008.65.
- [2] N. A. Macahig, "A 6-wire 3-phase inverter topology for improved BLDC performance and harmonics," in *2020 IEEE Applied Power Electronics Conference and Exposition (APEC)*, Mar. 2020, pp. 741–744, doi: 10.1109/APEC39645.2020.9124358.
- [3] P. Mishra, A. Banerjee, and M. Ghosh, "FPGA-based real-time implementation of quadral-duty digital-PWM-controlled permanent magnet BLDC drive," *IEEE/ASME Transactions on Mechatronics*, vol. 25, no. 3, pp. 1456–1467, Jun. 2020, doi: 10.1109/TMECH.2020.2977859.
- [4] Q. Liu, L. Guo, B. Gao, K. Ye, H. Chen, and H. Guo, "Coordinate receding horizon control for the power-shift process of multispeed electric vehicles," *IEEE Transactions on Vehicular Technology*, vol. 69, no. 1, pp. 1055–1059, Jan. 2020, doi: 10.1109/TVT.2019.2949469.
- [5] L. Zhang, Y. Wang, and Z. Wang, "Robust lateral motion control for in-wheel-motor-drive electric vehicles with network induced delays," *IEEE Transactions on Vehicular Technology*, vol. 68, no. 11, pp. 10585–10593, Nov. 2019, doi: 10.1109/TVT.2019.2942628.
- [6] B. Wang, P. Dehghanian, S. Wang, and M. Mitolo, "Electrical safety considerations in large-scale electric vehicle charging stations," *IEEE Transactions on Industry Applications*, vol. 55, no. 6, pp. 6603–6612, Nov. 2019, doi: 10.1109/TIA.2019.2936474.
- [7] D. Niculae, M. Iordache, M. Stanculescu, M. L. Bobaru, and S. Deleanu, "A review of electric vehicles charging technologies stationary and dynamic," in *2019 11th International Symposium on Advanced Topics in Electrical Engineering (ATEE)*, Mar. 2019, pp. 1–4, doi: 10.1109/ATEE.2019.8724943.
- [8] C. Chatzikomis, A. Sornioti, P. Gruber, M. Zanchetta, D. Willans, and B. Balcombe, "Comparison of path tracking and torque-vectoring controllers for autonomous electric vehicles," *IEEE Transactions on Intelligent Vehicles*, vol. 3, no. 4, pp. 559–570, Dec. 2018, doi: 10.1109/TIV.2018.2874529.
- [9] J. Han, A. Sciarretta, L. L. Ojeda, G. De Nunzio, and L. Thibault, "Safe- and eco-driving control for connected and automated electric vehicles using analytical state-constrained optimal solution," *IEEE Transactions on Intelligent Vehicles*, vol. 3, no. 2, pp. 163–172, Jun. 2018, doi: 10.1109/TIV.2018.2804162.
- [10] A. Rezaei, J. B. Burl, M. Rezaei, and B. Zhou, "Catch energy saving opportunity in charge-depletion mode, a real-time controller for plug-In hybrid electric vehicles," *IEEE Transactions on Vehicular Technology*, vol. 67, no. 11, pp. 11234–11237, Nov. 2018, doi: 10.1109/TVT.2018.2866569.
- [11] D. Zhang, G. Liu, H. Zhou, and W. Zhao, "Adaptive sliding mode fault-tolerant coordination control for four-wheel independently driven electric vehicles," *IEEE Transactions on Industrial Electronics*, vol. 65, no. 11, pp. 9090–9100, Nov. 2018, doi: 10.1109/TIE.2018.2798571.
- [12] C. Liu *et al.*, "Field circuit coupling analysis of dynamic wireless charging for electric vehicle," in *2018 IEEE 2nd International Electrical and Energy Conference (CIEEC)*, Nov. 2018, pp. 423–427, doi: 10.1109/CIEEC.2018.8745768.
- [13] A. Del Pizzo, M. Coppola, and I. Spina, "Current waveforms distribution among electrochemical cells of modular multilevel converters in battery electric vehicles," in *2018 IEEE International Conference on Electrical Systems for Aircraft, Railway, Ship Propulsion and Road Vehicles & International Transportation Electrification Conference (ESARS-ITEC)*, Nov. 2018, pp. 1–4, doi: 10.1109/ESARS-ITEC.2018.8607571.
- [14] J. Zhang, H. Yan, N. Ding, J. Zhang, T. Li, and S. Su, "Electric vehicle charging network development characteristics and policy suggestions," in *2018 International Symposium on Computer, Consumer and Control (IS3C)*, Dec. 2018, pp. 469–472, doi: 10.1109/IS3C.2018.00124.
- [15] M. O. Badawy, T. Husain, Y. Sozer, and J. A. De Abreu-Garcia, "Integrated control of an IPM motor drive and a novel hybrid energy storage system for electric vehicles," *IEEE Transactions on Industry Applications*, vol. 53, no. 6, pp. 5810–5819, Nov. 2017, doi: 10.1109/TIA.2017.2741438.




- [16] L. Samaranayake and S. Longo, "Degradation control for electric vehicle machines using nonlinear model predictive control," *IEEE Transactions on Control Systems Technology*, vol. 26, no. 1, pp. 89–101, Jan. 2018, doi: 10.1109/TCST.2016.2646322.
- [17] J. Zhu, K. W. E. Cheng, X. Xue, and Y. Zou, "Design of a new enhanced torque in-wheel switched reluctance motor with divided teeth for electric vehicles," *IEEE Transactions on Magnetics*, vol. 53, no. 11, pp. 1–4, Nov. 2017, doi: 10.1109/TMAG.2017.2703849.
- [18] V. P. Dhote, M. M. Lokhande, A. Agrawal, and B. H. Kumar, "Mechanical coupling of two induction motor drives for the applications of an electric-drive vehicle system," in *2017 National Power Electronics Conference (NPEC)*, Dec. 2017, pp. 330–333, doi: 10.1109/NPEC.2017.8310480.
- [19] A. Jaya, E. Purwanto, M. B. Fauziah, F. D. Murdianto, G. Prabowo, and M. R. Rusli, "Design of PID-fuzzy for speed control of brushless DC motor in dynamic electric vehicle to improve steady-state performance," in *2017 International Electronics Symposium on Engineering Technology and Applications (IES-ETA)*, Sep. 2017, pp. 179–184, doi: 10.1109/ELECSYM.2017.8240399.
- [20] J. J. Joseph, T. A. A. Victoire, M. C. Joseph, and F. T. Josh, "Axial flux permanent magnet motor-driven battery powered electric vehicle with zeta converter," in *2017 International Conference on Innovations in Electrical, Electronics, Instrumentation and Media Technology (ICEEIMT)*, Feb. 2017, pp. 353–358, doi: 10.1109/ICEEIMT.2017.8116865.
- [21] A. Saleki, S. Rezaade, and M. Changizian, "Analysis and simulation of hybrid electric vehicles for sedan vehicle," in *2017 Iranian Conference on Electrical Engineering (ICEE)*, May 2017, pp. 1412–1416, doi: 10.1109/IranianCEE.2017.7985263.
- [22] F. Naseri, E. Farjah, and T. Ghanbari, "An efficient regenerative braking system based on battery/supercapacitor for electric, hybrid and plug-in hybrid electric vehicles with BLDC motor," *IEEE Transactions on Vehicular Technology*, vol. 66, no. 5, pp. 3724–3738, 2016, doi: 10.1109/TVT.2016.2611655.
- [23] M. S. Alam Chowdhury, K. A. Al Mamun, and A. M. Rahman, "Modelling and simulation of power system of battery, solar and fuel cell powered hybrid electric vehicle," in *2016 3rd International Conference on Electrical Engineering and Information Communication Technology (ICEEICT)*, Sep. 2016, pp. 1–6, doi: 10.1109/CEEICT.2016.7873126.
- [24] X. Sun, C. Shao, G. Wang, L. Yang, X. Li, and Y. Yue, "Research on electrical brake of a series-parallel hybrid electric vehicle," in *2016 World Congress on Sustainable Technologies (WCST)*, Dec. 2016, pp. 70–75, doi: 10.1109/WCST.2016.7886594.
- [25] P. Sarala, S. F. Kodad, and B. Sarvesh, "Analysis of closed loop current controlled BLDC motor drive," in *2016 International Conference on Electrical, Electronics, and Optimization Techniques (ICEEOT)*, Mar. 2016, pp. 1464–1468, doi: 10.1109/ICEEOT.2016.7754925.
- [26] A. Varshney and B. Dwivedi, "Performance analysis of a BLDC drive under varying load," in *2016 IEEE 1st International Conference on Power Electronics, Intelligent Control and Energy Systems (ICPEICES)*, Jul. 2016, pp. 1–4, doi: 10.1109/ICPEICES.2016.7853626.

BIOGRAPHIES OF AUTHORS



Nagaraja Rao    received a B.E. degree in electrical and electronics engineering and M.Tech. in microelectronics and control systems from NMAMIT, Nitte in 2003 and 2005, respectively. He is working as an associate professor in the Department of ECE at SMVITM, Bantakal. Prior to joining SMVITM, he was working as an assistant professor in EEE Department at The Oxford College of Engineering Bangalore. He is having a total of 16 years of teaching experience. Presently, he is pursuing his Ph.D. in the area of control engineering under the guidance of Dr. Shantharama Rai, Principal, AJIET, Mangalore. His areas of interest are control engineering, modern control engineering, circuit theory, and digital signal processing. He is a life member of ISTE and ISTD. He has published/presented around 10 papers in international/national journals/conferences in the field of engineering. He can be contacted at nagarajsmvitm1@gmail.com.



Shantharama Rai Chelladka    completed his Bachelor of Engineering (B.E.) from Mangalore University, M.Tech. from N.I.T.K. Surathkal, and Ph.D. from V.T.U. Belgaum with a specialization in power electronics and control systems. He is also a member of Indian Society for Technical Education, New Delhi, and Indian Society for Lighting Engineers, New Delhi. He has served in different institutions/organizations like K.V.G. College of Engineering, Sullia, N.M.A.M. Institute of Technology, Nitte, St. Joseph Engineering College Vamanjoor, and Canara Engineering college Mangalore in various capacities for more than 18 years. He has published/presented more than 40 papers in international/national journals/conferences in the field of engineering. He has guided more than 50 UG projects, and more than 15 PG projects. Presently, he is guiding 7 Ph.D. students. The project guided by him titled Generation of Electric Power from Waste Products Using Specially Designed Spark Ignition Engine is awarded as the quality of very high order and obtained the certificate of commendation from Karnataka State Council for Science and Technology, Indian Institute of Science Bangalore. He also obtained more than 35 lacs grant for his research work from VTU and AICTE New Delhi. Dr. Shantharama Rai C. has participated in and presented a research paper in the state of Kuwait. He was the coordinator for the Mangalore Region to assess the Quality of Electrical Distribution Governance and Performance in Karnataka (MESCOM Region) appointed by K.S.C.S.T Bangalore for the year 2007-2008. He is also an executive member of different organizations in Mangalore and serves to the public through many organizations. Dr. Rai was also a member of Ph.D. candidate selection, a member of the examination committee (BOE), and the local inspection committee of Visvesvaraya Technological University Belgaum Karnataka. He can be contacted at principal@ajiet.edu.in.